

$$I = 2\pi(\hbar c)^5 \int_0^\infty \int_{-1}^1 dy d\mu_0 y^2 \exp[-\alpha y - i p y \mu_0] [I_x(\alpha; y) - I_x(2\alpha; y)], \quad (7A)$$

where

$$I_x(\alpha; y) \equiv 2\pi \int_0^\infty x^2 dx e^{-\alpha x} \int_{-1}^1 d\mu [x^2 + y^2 - 2xy\mu]^{-\frac{1}{2}}. \quad (8A)$$

In writing the results of the  $\mu$  integration in Eq. (8A), they must be arranged so that the factor  $(x-y)$  will always be greater than zero since  $|x-y| > 0$ . Thus it can be shown that

$$I_x(\alpha; y) = 4\pi \left[ \left(\frac{1}{y}\right) \int_0^y x^2 e^{-\alpha x} dx + \int_y^\infty x e^{-\alpha x} dx \right], \quad (9A)$$

$$I_x(\alpha; y) = (4\pi/y) [2/\alpha^3 - (y/\alpha^2)e^{-\alpha y} - (2/\alpha^3)e^{-\alpha y}]. \quad (10A)$$

Upon substituting Eq. (10A) in Eq. (7A) and performing the  $\mu_0$  integration, the result will be

$$I = \left[ \frac{(4\pi)^2 (\hbar c)^5}{\alpha^2 p} \right] \int_0^\infty dy \sin p y e^{-\alpha y} \left\{ \left[ \frac{2}{\alpha} - y e^{-\alpha y} - \frac{2}{\alpha} e^{-\alpha y} \right] - \left[ \frac{1}{\alpha} - y e^{-2\alpha y} - \frac{1}{\alpha} e^{-2\alpha y} \right] \right\}. \quad (11A)$$

When the  $y$  integration in Eq. (11A) has been performed,  $I$  will take the explicit form

$$I = \left[ \frac{2(4\pi)^2 (\hbar c)^5}{\alpha} \right] \left[ \frac{p^2 + 10\alpha^2}{(p^2 + \alpha^2)(p^2 + 4\alpha^2)} - \frac{2p^2 + 33\alpha^2}{(p^2 + 4\alpha^2)(p^2 + 9\alpha^2)} \right]. \quad (12A)$$

Upon using the results of Eq. (12A) and the substitutions of Eq. (5A) in Eq. (1A), the result can be brought into the form of Eq. (4) of the text.

## Superconducting Transition in Aluminum\*

JOHN F. COCHRAN† AND D. E. MAPOTHER

*Physics Department, University of Illinois, Urbana, Illinois*

(Received February 19, 1958)

Further results on the superconducting properties of aluminum are given which supplement those previously reported. The critical field curve for pure Al has been measured by using a paramagnetic salt as a thermometer. Except for a region very near  $T_c$ , our data are accurately represented by the parabolic relation,  $H_c = H_0[1 - (T/T_c)^2]$ , where  $T_c = 1.196 \pm 0.005^\circ\text{K}$  and  $H_c$  is about  $99 \pm 1$  gauss. The excellent reproducibility of the  $S$ - $N$  transition in Al suggests that it may serve as a useful secondary thermometric standard near  $1^\circ\text{K}$ . Further observations are reported on the broadening tendency of magnetically measured transitions in single-crystal specimens near  $T_c$ . It is also found that polycrystalline specimens of the same material do not show the broadening effect. A semiquantitative theory of the intermediate state is applied to explain the observation that the magnetic transition is sharper than predicted on the basis of specimen geometry at temperatures well below  $T_c$ . The difference in sharpness can be explained as a contribution of the interphase free energy whose order of magnitude has been estimated with fair success from the observed shape of the magnetic transition.

### I. INTRODUCTION

IN a previous article<sup>1</sup> (to be referred to hereafter as I) a cryostat was described for investigating the superconducting transition in metals having critical temperatures down to about  $0.8^\circ\text{K}$ . Although the cryostat was found to be very satisfactory for studying the properties of the transition at constant temperature, a carbon resistor was used as a thermometer and our experience indicated that the resistance-temperature relationship for such resistors could not be reliably extrapolated to temperatures below our calibration range of  $1.5$ – $4.2^\circ\text{K}$ . Because of the lack of a reliable thermometric element,

it was decided to redesign the inner helium container of the cryostat described in I so as to incorporate into it a paramagnetic salt pill. The use of this modified cryostat to measure the temperature dependence of the critical field in pure aluminum is reported herein.

The attempt in the present work has been to obtain precise information about the critical-field curve of pure Al. Previous study of the superconducting transition under isothermal conditions has shown that the  $S$ - $N$  transition in pure aluminum is very reproducible from specimen to specimen. Thus accurate measurements of the critical field curve, in addition to yielding information about the properties of Al, may also provide a practical secondary thermometric standard for a range in which absolute temperature determinations are difficult.

\* Assisted by the Office of Ordnance Research, U. S. Army.

† Present address: Physics Department, Massachusetts Institute of Technology, Cambridge, Massachusetts.

<sup>1</sup> Cochran, Mapother, and Mould, *Phys. Rev.* **103**, 1657 (1956).

## II. APPARATUS AND PROCEDURE

### A. The Cryostat

The cryostat and solenoids described in I were used in these experiments, and the same measuring techniques were employed. The only change was in the design of the inner helium chamber.

A diagram of the modified inner vessel is shown in Fig. 1. The specimen chamber ( $S$ ) is loaded through the removable plug ( $K$ ) which is sealed with a nonsuperconducting soft solder.<sup>1</sup> Liquid helium from the main body of the pot flows through holes in the upper part of each tube  $S$  to fill the sample chambers. The salt pill,  $A$ , is contained in a 4-inch long,  $\frac{1}{2}$ -inch diameter brass tube, closed at each end, and supported from the bottom so that it is coaxial with a second brass tube of slightly larger diameter. The inner tube is filled from the bottom by means of a removable screw cap. The upper end of the outer tube opens directly into the inner pot so that the salt pill is surrounded by a sheath of liquid helium ( $H$ ). It is our experience that this sheath must be generously proportioned if the salt pill is to remain in thermal equilibrium with the helium bath. In early designs, where the radial clearance for helium was under 0.010 inch, the salt pill temperature was frequently observed to differ appreciably from the bath temperature because of magnetic heating in the process of measuring a superconducting transition. No such difficulties were experienced with the design shown in Fig. 1 where the radial clearance was about 0.030 inch.

It was necessary to encase the salt pill in a vacuum-tight container in order to prevent its dehydration when evacuating the inner vessel. Evacuation of the inner vessel was necessary during cool-down in order to keep the orifice clean of condensable vapors.

$C$  is a copper sleeve into which the carbon resistance thermometer is screwed, and which is machined with fins to improve the thermal contact with the helium bath. The helium in the inner vessel is pumped through the orifice  $O$  and the  $\frac{1}{4}$ -inch diameter 0.006-inch thick wall Inconel tubing  $P$ . The orifice is a half-inch length of  $\frac{1}{16}$ -inch outer diameter, 0.004-inch thick wall Inconel tubing soldered into the nipple ( $N$ ). A 300-ohm heater coil was wound directly on the upper end of the vessel (not shown in the diagram).

Because of space limitations the pickup coils  $X$ ,  $Y$  and dummy coils  $D_X$ ,  $D_Y$  could not be thermally isolated from the inner vessel, as in I, but had to be attached directly to the sample tubes and salt pill tail as shown in Fig. 1. The electrical leads were wrapped around and cemented to the pumping tube  $P$  to reduce heat leakage. However, the heat leak was always greater than in the apparatus described in I, and the ultimate stable temperature obtainable with this vessel was about 0.85°K. The temperature of the inner vessel was stabilized to better than  $\pm 10^{-4}$ °K by the same procedure described in I.

The salt pill was made up of a mixture of potassium-

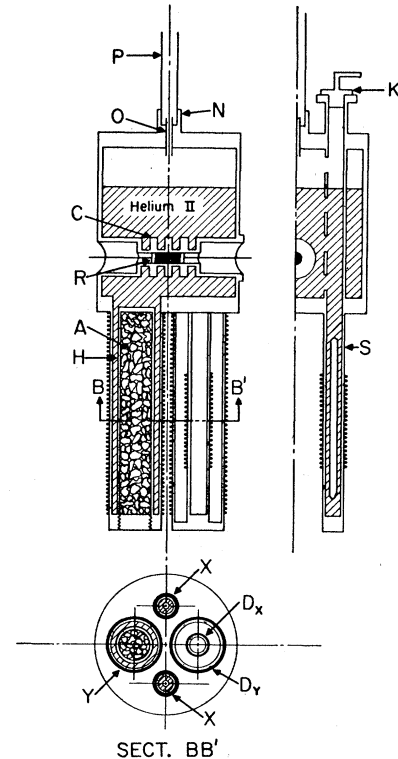


FIG. 1. Schematic cross section of the inner helium vessel containing the specimens and salt pill. This vessel was suspended within the vacuum jacket of the apparatus described in I.

chrome-alum crystals (approximately 1 mm on a side) and Araldyte AN-102. The Araldyte served to bind the crystals of alum together to provide thermal contact with each other and with the walls of the salt pill chamber. A  $\frac{1}{8}$  inch thick copper strip ran through the center of the salt pill and was soldered to the walls of the salt pill container to reduce the length of the maximum thermal conduction path.

### B. Temperature Determination

The susceptibility of the salt pill was measured by means of the coil  $Y$ , Fig. 1, and the identical dummy coil  $D_Y$  connected in series opposition through a galvanometer and the secondary of a variable mutual inductor. The primary of the mutual inductor was connected in series with the air solenoid. The galvanometer deflection was measured as a function of the external mutual inductance setting when an air solenoid field of 5 gauss was quickly turned off. In this way curves were obtained which could be fitted by least squares to a linear function of the form  $\delta = a + bM$ . For  $\delta = 0$ , one has  $M_0 = -a/b$ , where  $M_0$  is the desired value of mutual inductance. In this way  $M_0$  could be determined with a precision of about  $\pm \frac{1}{2}$  microhenry, and this quantity is proportional to the susceptibility of the salt pill. The total variation in  $M_0$  between 4°K and 0.845°K was 460  $\mu$ h.

In order to calibrate the salt pill, the inner bath was sealed off from the pumps and connected to a mercury manometer, while the jacket insulating the inner from

the outer bath was flooded with helium gas. With the outer bath stabilized at the desired temperature, simultaneous values of the vapor pressure over the helium in the inner vessel and the salt pill mutual inductance were recorded. The vapor-pressure readings were translated into temperatures by means of the vapor-pressure tables prepared at the Naval Research Laboratory on the basis of the vapor-pressure equation proposed by Clement, Logan, and Gaffney.<sup>2</sup> Vapor pressures above the  $\lambda$  point were corrected for a 12-cm hydrostatic head of helium above the salt pill. As shown in Fig. 1, the apparatus also carried a carbon resistance thermometer in good thermal equilibrium with the inner helium bath and the salt pill. Its values were recorded as a further check on the temperature. Calibration points were measured throughout a temperature region extending from about 1.5 to 4°K.

### C. Superconductivity Measurements

During the measurements each search coil was connected in series opposition with the dummy coil through the 600-ohm critical damping resistance galvanometer as described in I. The interpretation of galvanometer response in terms of flux penetration into the superconducting specimen has also been described in I, and applies in the present case. The essential point is that the magnetic field is increased monotonically through the transition in discrete steps of approximately 0.08 gauss each. The average magnetic induction of the specimen, expressed as the effective permeability  $\mu_e$ , is determined from the ballistic deflections of the galvanometer which accompany each stepwise change in the external magnetic field.

### D. The Specimens

The specimen blanks were cylinders 2 inches long,  $\frac{1}{8}$  inch in diameter, and pointed at one end to promote nucleation for single-crystal growth. The blanks were machined from 99.99% pure aluminum bar stock supplied by the Aluminum Corporation of America, and grown into single crystals using the soft mold technique of Noggle<sup>3</sup> in conjunction with the Bridgman method for growing crystals.<sup>4</sup> Grain boundaries were made visible by means of a macro-etch due to Beck *et al.*<sup>5</sup> Polycrystals of three different grain sizes were produced by heat treating the blanks at 550°C for one, two, and four hours. This treatment yielded specimens with average grain sizes of 1 mm, 2 mm, and 4 mm, respectively. The specimens used for this investigation are listed in Table I.

Several of the specimens were investigated after having their surfaces polished by means of the Alcoa

R5 Bright Dip chemical polish. The polished surfaces appeared to be smooth under a magnification of 50 000.

The specimens were centered in the sample chambers by means of Lucite caps. The caps fitted the cylinders sufficiently loosely so that they did not pinch the crystals when the apparatus was cooled to 4°K.

## III. RESULTS

### A. Superconducting to Normal Transition

As discussed in I it is convenient to display the transition from the superconducting to the normal state at constant temperature in terms of the effective permeability,  $\mu_e$ , where  $\mu_e$  is essentially the average magnetic induction within the specimen divided by the critical field. For an ellipsoidal specimen whose dimensions are very large compared to the penetration depth,  $\lambda \sim 10^{-6}$  cm, the effective permeability should be given by

$$\mu_e = 1 - \frac{1}{n}(1-h),$$

where  $n$  is the demagnetizing coefficient characteristic of the axis along which the field is directed, and  $h = H_e/H_c$  is the ratio of the applied field to the critical

TABLE I. Characteristics of specimens measured.

Specimen	Structure	Physical characteristics
7	Single crystal	
10	Single crystal	
18	Single crystal	
19	Single crystal	
27	Polycrystal	1 mm average grain size
28	Polycrystal	2 mm average grain size
29	Polycrystal	4 mm average grain size

field. In the ideal case  $\mu_e$ , when plotted as a function of  $h$ , should be a straight line passing through the point ( $\mu_e=1, h=1$ ) with a slope equal to the reciprocal of the demagnetizing coefficient.

Although the specimens used in these experiments were cylinders rather than ellipsoids it is to be expected that they can be characterized by a demagnetizing coefficient equal to that of an ellipsoid having the same ratio of length to diameter. In the present case this ratio is 16:1, and from Stoner's tabulation<sup>6</sup> the value for this ellipticity is  $n=0.0097$ .

In Figs. 2(a) and 2(b) are shown graphs of  $\mu_e$  versus  $h = H_e/H_c$  for single crystal 7 for a number of temperatures. Similar results were obtained for the other single crystals and, in agreement with the results reported in I for an accurately ellipsoidal specimen, the curves reveal deviations from the expected ideal behavior in three respects.

(1) The points for sufficiently low temperatures [Fig. 2(b)] do indeed follow a straight line as  $\mu_e$

<sup>6</sup> E. C. Stoner, *Phil. Mag.* **36**, 803 (1945).

<sup>2</sup> Clement, Logan, and Gaffney, *Phys. Rev.* **100**, 743 (1955).

<sup>3</sup> T. S. Noggle, *Rev. Sci. Instr.* **24**, 184 (1953).

<sup>4</sup> P. W. Bridgman, *Proc. Am. Acad. Arts Sci.* **60**, 305 (1925).

<sup>5</sup> Beck, Kremer, Demer, and Holzworth, *Trans. Am. Inst. Mining Met. Engrs.* **175**, 372 (1948).

approaches unity, but a straight line corresponding to a smaller demagnetizing coefficient than that calculated from the specimen geometry. In the present instance the four single-crystalline specimens appear to have an average effective demagnetizing coefficient of  $n_e=0.008$ .

The tailing off of the points at low-field values indicates that the field begins to penetrate into the specimen sooner than would be expected for an ideal ellipsoid, and seems to be caused by the deviation from ellipsoidal geometry. Similar curves for accurately ellipsoidal specimens do not show such pronounced rounding near  $\mu_e=0$ .

(2) As the temperature approaches the critical temperature, i.e., for small  $H_c$ , the permeability curves become rounded over as  $\mu_e$  approaches unity [Fig. 2(a)]. Under these circumstances it becomes difficult to decide what exactly is the critical field, so that the following

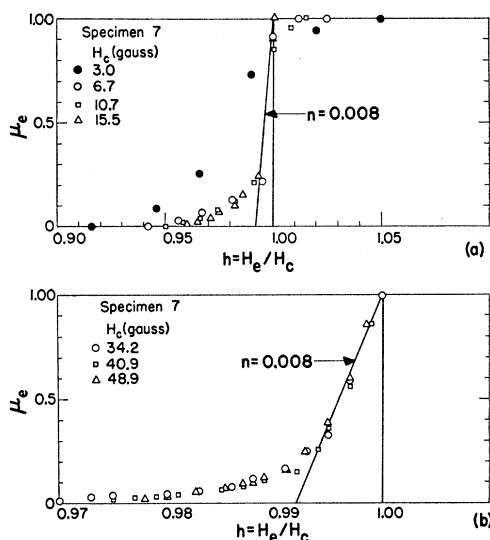


FIG. 2. (a) Effective permeability,  $\mu_e$ , as a function of the reduced field,  $h$ , for single crystal 7 at temperatures near the critical temperature. (b)  $\mu_e$  vs  $h$  for single crystal 7 at temperatures well below the critical temperature.

nomenclature was adopted in I and also used here; the linear portion of a given  $\mu_e$  versus  $H_e$  curve was extrapolated to intersect the line  $\mu_e=1$  at that value of the external field defined as the critical field. A further field,  $H_n$ , was introduced in I, and defined as that value of the external field for which the transition was completed. Experimentally speaking,  $H_n$  could be determined with a precision which was limited only by the magnitude of the step-intervals in the magnetic field (0.08 gauss in the present case) used to traverse a transition. Because of the gradual smearing out of the transition curves as the temperature approached  $T_c$ , it was hard to determine  $H_c$  with the same precision as  $H_n$ ; but within experimental accuracy the difference,  $H_n - H_c$ , was the same for each single crystal at a given temperature, was zero for temperatures less than about

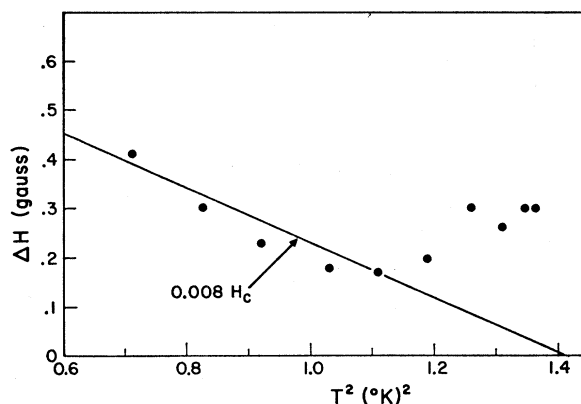


FIG. 3. Transition width for single-crystal specimen 7 as a function of the square of the temperature. The straight line gives the ideal transition width for a specimen having a demagnetizing coefficient of  $n=0.008$ . Similar behavior was seen for all the other single-crystal specimens.

1 $^{\circ}\text{K}$ , and appeared to increase to a maximum value of roughly 0.15 gauss near  $T_c$ . The difference,  $H_n - H_c$ , and therefore the shape of the transition curves, appeared to be unaffected by surface treatment or handling of the specimens.

(3) For temperatures approaching the critical temperature, the transition takes place over a much broader magnetic field interval than predicted for the ideal transition. The tailing off near  $\mu_e=0$  makes it difficult to determine precisely the breadth of a given transition, but if one extrapolates the linear portion of a  $\mu_e$  versus  $H_e$  plot to  $\mu_e=0$  and calls the field interval between this intercept and  $H_n$  the transition width,  $\Delta H$ , such an interval should be a reasonable measure of the breadth to be expected for an equivalent ellipsoid. As can be seen from Fig. 3, the transition width goes through a minimum in the neighborhood of 1.05 $^{\circ}\text{K}$ . On a  $T^2$  plot, the ideal transition width to be expected for an ellipsoid with a demagnetizing coefficient of 0.008 is the straight line shown in the diagram.

In marked contrast with the single crystals, the polycrystalline specimens exhibited the ideal behavior over

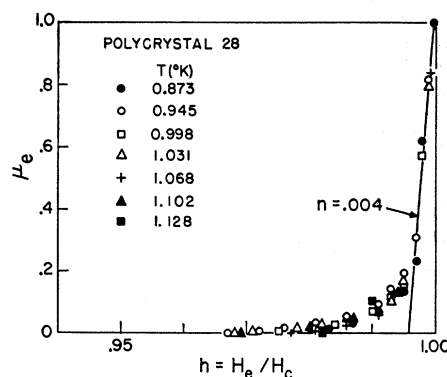


FIG. 4.  $\mu_e$  vs  $h$  for polycrystal 28 at various temperatures. Note that the broadening effect apparent in Fig. 2(a) does not occur with the polycrystalline specimen.

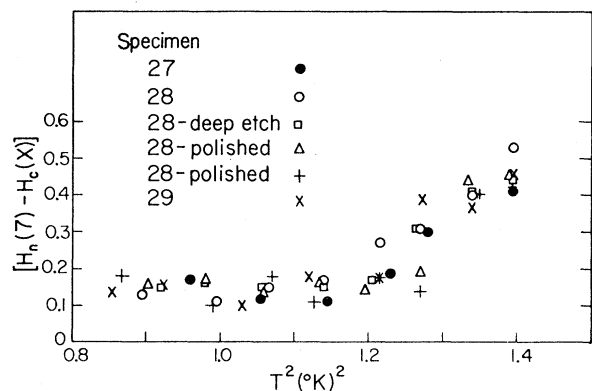


FIG. 5. Difference between  $H_n$  for single crystal 7 and  $H_c$  for several polycrystalline specimens shown as a function of the square of the temperature.

the whole temperature range, with the exception that each polycrystal behaved as if it had a demagnetizing coefficient of  $n_e=0.004$  instead of the calculated value of 0.0097. Curves of  $\mu_e$  versus  $h=H_c/H_c$  are shown in Fig. 4 for specimen 28. The curves for the other two polycrystals were practically identical with those shown in Fig. 4. Within experimental error the transition width,  $\Delta H$ , was linear with  $H_c$  over the whole temperature interval. For instance, at  $H_c=0.6$  gauss the transition in the polycrystals occurred within one step-width of 0.08 gauss, the limiting resolution of the apparatus.

In order to obtain an idea of the reproducibility of the superconducting transition from specimen to specimen, runs were made in which each of the other specimens were measured simultaneously with crystal 7.  $H_n$  and  $H_c$  were the same for single crystals 7, 10, and 19 to within 0.1 gauss over the whole temperature range.  $H_c$  and  $H_n$  for single crystal 18 were consistently 0.3 gauss smaller than those for specimen 7.<sup>7</sup> In Fig. 5 are shown the results of the measurements for the polycrystalline specimens in the form of the difference between  $H_n$  for crystal 7 and the critical field for each polycrystal. The critical fields appear to be the same for all of the polycrystals over the whole temperature interval to within 0.1 gauss, i.e., to within the resolution of the apparatus. The rise exhibited by the points in Fig. 5 as  $T_c$  is approached is due to the broadening of the transition in crystal 7 near  $T_c$  discussed above and shown in Fig. 3.

Clearly more data would be desirable, but in view of

<sup>7</sup> This statement is based on three comparison observations made at the conclusion of the present work. At critical fields of about 7, 19, and 35 gauss, shifts in critical field were respectively 0.30, 0.27, and 0.28 gauss with specimen 18 having in every case the smaller  $H_c$ . These shifts are clearly outside the limit of resolution of the measuring method and, therefore, this particular result is at variance with the generally excellent agreement between  $H_c$  values observed in all other comparison measurements. The fact that this shift is independent of temperature suggests that it may originate in a strained condition in one of the specimens, but, in view of the consistency of the overwhelming majority of the data, no further study of this particular anomaly was made.

the sharpness of their transitions and the reproducibility from specimen to specimen, the possibility presents itself of using the superconducting transition in polycrystalline aluminum specimens as a secondary thermometer. For Al one can write approximately

$$H_c \approx 100(1 - T^2/1.43);$$

therefore

$$\Delta T \approx \Delta H_c / (140T).$$

An uncertainty in  $H_c$  of 0.2 gauss would still suffice to fix the absolute temperature to within 0.003°K at 0.5°K. If other superconductors in the range between 0.1 and 1°K were found to have sharp, reproducible transitions, they could also be used to provide a number of secondary temperature points for calibration purposes. At the present time the paramagnetic salts used for thermometry below 1°K must be calibrated against the vapor pressure of liquid helium, a procedure which is always long and tedious.

In connection with the above possibility, it should be mentioned that it is desirable to leave the specimens with an etched surface in order to provide points of nucleation for the growth of the normal phase. The single crystals invariably displayed evidence of some superheating when polished, although this usually manifested itself as a delayed entry into the intermediate state rather than as an increase in the critical field. One polycrystal (27) showed a very large superheating effect when polished. The effect was a maximum in the neighborhood of 1.1°K where the transition took place directly from the superconducting to the normal state within an interval of 0.08 gauss and at fields of the order of 1.5 gauss greater than the critical field for the same specimen with an etched surface.

## B. Temperature Dependence of the Critical Field

In I we tried to extrapolate the  $R$  versus  $T$  equation of a carbon resistor calibrated against the vapor pressure of liquid He, but the empirical nature of the  $R$  dependence upon  $T$  makes this a dubious procedure if temperature values are needed beyond the limits of the calibration range. In the present work we have used the susceptibility of potassium chrome alum as the thermometric parameter. Again it has been necessary to determine temperatures beyond the limit of the calibration range, but the paramagnetic salt thermometer has the advantage over the more convenient carbon thermometer that there exists a substantial theoretical basis for deriving an analytic relation between the susceptibility and the absolute temperature. We hoped to obtain the temperature dependence of  $H_c$  with sufficient accuracy to permit its use to standardize other temperature measurements near 1°K.

The experimental procedure followed in determining the temperature magnetically has been described above. Table II gives the results of the calibration measure-

ments on two separate experimental runs, where  $M_0$  is the mutual inductance of the coil system containing the salt pill and  $T$  is the corrected absolute temperature determined from simultaneous measurements of the vapor pressure of liquid He. The susceptibility of potassium chrome alum should follow a Curie-Weiss law which, in terms of the observable  $M_0$ , may be written as

$$M_0 = A - B/(T - \Delta), \quad (1)$$

where  $T$  is the absolute temperature,  $\Delta$  is the Curie-Weiss constant, and  $A$  and  $B$  are constants depending upon specimen and coil geometry and the susceptibility of the salt.<sup>8</sup>

In fitting the calibration data to Eq. (1),  $\Delta$  was computed from the relation

$$\Delta = \frac{4}{3}\pi fC = 0.017^\circ\text{K}, \quad (2)$$

where  $f=0.6$  is the filling factor for the salt pill (i.e., the ratio of the mass of salt contained in one cc to the density of the crystalline salt), and  $C=6.71 \times 10^{-3}$  emu is the Curie constant per cc for potassium chrome alum. In calculating the above value of  $\Delta$ , it is assumed that the individual salt crystals were randomly oriented. If this were not the case, the value of  $\Delta$  might be in error by as much as a factor or two, but, fortunately, it turns out that temperatures calculated from calibration data fitted to an equation of the form of (1) are not sensitive to changes in  $\Delta$ . Having determined  $\Delta$ ,

TABLE II. Magnetic thermometer calibrations.

Obs. No.	Run 1:			Run 2:		
	$p^a$ (mm Hg)	$T^b$ (°K)	$M^c$ ( $\mu\text{h}$ )	$p^a$ (mm Hg)	$T^b$ (°K)	$M^c$ ( $\mu\text{h}$ )
1	319.2	3.408	145.4	584.6	3.944	152.4
2	177.6	2.980	126.3	473.3	3.745	146.7
3	103.6	2.652	106.8	362.0	3.511	139.0
4	26.30	2.034	56.9	287.7	3.326	133.1
5	566.9	3.914	158.8	219.1	3.124	125.2
6	413.2	3.624	151.0	179.2	2.986	117.9
7	287.0	3.324	138.8	150.7	2.874	112.3
8	198.2	3.054	127.4	120.0	2.736	105.5
9	206.0	3.081	128.4	99.4	2.629	98.5
10	142.2	2.839	116.8	80.3	2.516	90.9
11	108.5	2.678	107.2	68.4	2.436	86.2
12	79.70	2.512	96.8	54.6	2.329	77.7
13	60.28	2.375	86.7	47.3	2.266	72.9
14	43.41	2.229	73.9	34.75	2.138	61.8
15	36.60	2.158	66.9	27.35	2.048	54.0
16	30.17	2.084	59.8	24.36	2.008	49.4
17	10.02	1.740	17.7	19.39	1.932	41.2
18	18.29	1.914	41.3	13.24	1.817	24.9
19	9.89	1.737	17.8	7.46	1.668	7.0
20	13.81	1.829	30.9	5.69	1.604	-2.7
21	14.19	1.837	32.3	15.81	1.869	31.3
22	252.6	3.227	135.2	10.84	1.761	18.5
23	54.13	2.325	82.0			

<sup>a</sup> Values of  $p$  are observed vapor pressures of He bath corrected for hydrostatic head, gravity, and temperature of mercury manometer.

<sup>b</sup> Values of  $T$  are obtained from the  $T_{\text{He}}$  scale of Clement, Logan, and Gaffney, reference 2. See their note added in proof.

<sup>c</sup> Least-squares fit to  $M = A - B/(T - 0.017)$  gives for Run 1:  $A = 272.03$ ,  $B = 437.33$ ; for Run 2:  $A = 262.64$ ,  $B = 426.71$ .

<sup>8</sup> D. De Klerk, *Handbuch der Physik* (Springer-Verlag, Berlin, 1955), Vol. 15, p. 38.

TABLE III. Critical-field data.

Run 1:				Specimen 18		Specimen 19	
Obs. No.	$M$ ( $\mu\text{h}$ )	$T$ (°K)	$T^2$	$H_c$ (gauss)	$H_s$ (gauss)	$H_c$ (gauss)	$H_s$ (gauss)
II	-220.2	0.906	0.820	42.02	29.2	42.07	25.00
III	-192.7	0.958	0.918	34.93	22.9	35.17	19.5
IV	-172.0	1.002	1.004	28.52	17.2	28.54	14.5
V	-157.6	1.035	1.071	24.48	14.1	24.34	11.5
VI	-141.8	1.074	1.153	18.82	9.4	18.77	8.4
VII	-130.9	1.102	1.215	14.53	6.1	14.68	5.9
VIII	-120.4	1.131	1.280	10.33	3.9	10.15	4.0
IX	-108.9	1.165	1.356	5.12	1.6	5.22	1.9
X(a)	-100.5	1.191	1.419	...	...	1.18	...
X	-98.5	1.197	1.434	1.14	<0.1	1.11	0.1
XI	-114.2	1.149	1.321	7.42	2.7	7.57	2.7
XII	-124.6	1.120	1.254	12.52	5.2	12.70	5.1
XIII	-135.4	1.090	1.189	16.57	7.8	16.77	7.4
XIV	-202.6	0.938	0.881	37.54	25.2	37.67	24.3

Run 2:				Specimen 7		Specimen 10	
Obs. No.	$M$ ( $\mu\text{h}$ )	$T$ (°K)	$T^2$	$H_c$ (gauss)	$H_s$ (gauss)	$H_c$ (gauss)	$H_s$ (gauss)
I	-193.1	0.953	0.909	36.46	19.5	36.53	19.5
II	-223.0	0.896	0.802	43.93	25.6	44.04	26.8
III	-239.9	0.866	0.750	47.56	28.6	47.58	29.3
IV	-204.9	0.930	0.864	39.50	22.0	39.66	23.8
V	-171.1	1.001	1.002	29.77	14.4	29.90	17.4
VI	-180.9	0.979	0.959	32.88	16.8	32.94	19.3
VII	-156.4	1.035	1.072	24.84	10.6	24.93	14.3
VIII	-142.0	1.072	1.148	19.56	8.1	19.65	11.6
IX	-128.2	1.109	1.229	14.13	5.5	14.16	8.9
X	-117.2	1.140	1.301	9.39	3.1	9.35	6.3
XI	-104.3	1.180	1.392	4.01	...	4.01	2.8
XII	-135.8	1.088	1.184	17.25	7.0	17.32	10.5
XIII	-99.2	1.196	1.431	1.39	0.2	1.28	0.4
XIV	-99.0	1.197	1.433	1.26	<0.1	1.15	0.4
XV	-102.0	1.187	1.409	3.06	...	3.05	...
XVI	-109.3	1.164	1.355	6.77	2.3	6.81	4.6
XVII	-123.6	1.122	1.258	12.13	4.3	12.17	7.8

the calibration data were subjected to a least-squares analysis to determine the best values for  $A$  and  $B$  for each run. The resulting calibration constants are given in Table II. For reasons discussed below, we estimate that the over-all accuracy achieved in the extrapolation of these calibration equations is of the order of  $0.005^\circ\text{K}$ .

As described in more detail in I, the procedure followed in measuring critical fields was to stabilize the cryostat temperature at various points in the superconducting region, and for each stabilized temperature to observe the variation of  $\mu_e$  with applied field for each specimen as well as the equilibrium value of  $M_0$  for the salt pill. In each of the two runs for which an accurate salt pill calibration was made, two different pure single crystals were present in the apparatus (specimens 18 and 19 in the first run and specimens 7 and 10 in the second). The data obtained are presented in Table III together with  $T^2$  and  $T$  values deduced from the appropriate salt pill calibration equation. The  $H_s$  values listed for each specimen are the values of external field for which the supercooled transition occurred. The  $H_c$  values are shown graphically in Fig. 6 as a function of  $T^2$ .

Within the accuracy of the present measurements  $H_c$  has a parabolic dependence on  $T$  over most of the range

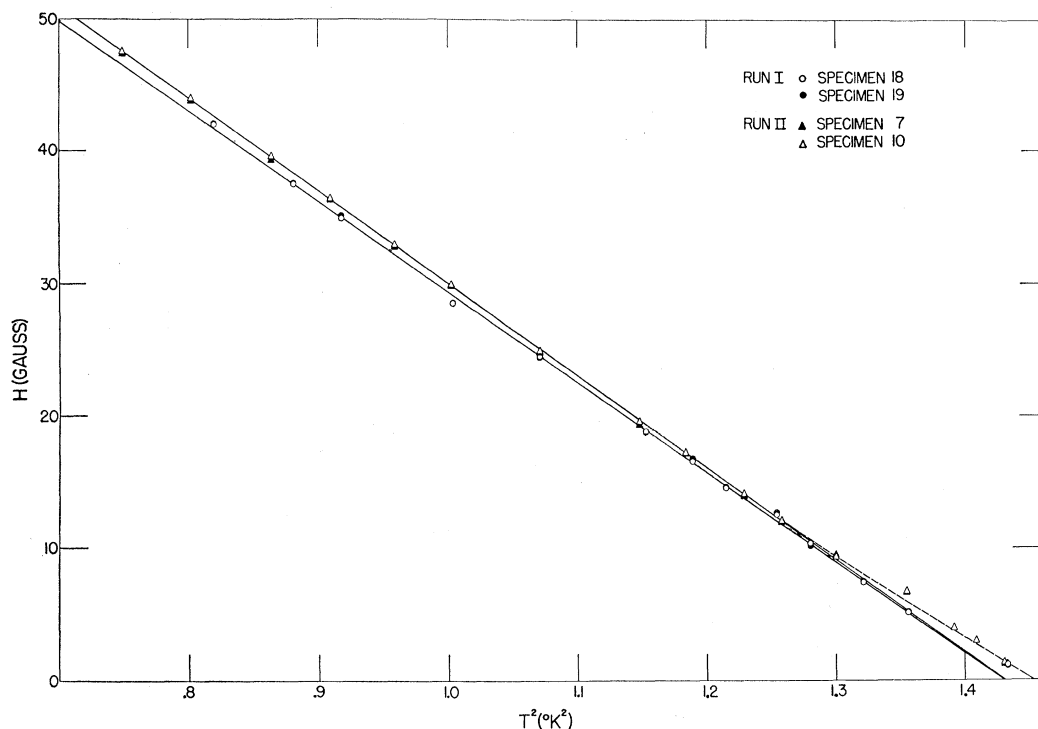


FIG. 6. Critical-field values of the single-crystal specimens as a function of  $T^2$ . The two straight lines represent Eq. (3) with the constants given in the text. Note tendency of experimental points as  $H_c \rightarrow 0$ .

of temperature studied. Below about  $1.12^\circ\text{K}$  the data of the two runs are accurately represented by the formula,

$$H_c = H_0[1 - (T/T_c)^2], \quad (3)$$

where, for Run 1,

$$H_0 = 97.8 \text{ gauss}, \quad T_c = 1.196^\circ\text{K},$$

and, for Run 2,

$$H_0 = 100.0 \text{ gauss}, \quad T_c = 1.196^\circ\text{K}.$$

The difference in  $H_0$  values for the different runs is almost certainly a sole consequence of the inaccuracies introduced in extrapolating the absolute temperature. The difference between the two curves of Fig. 6 at the lowest temperature could be explained by an error of about 8 millidegrees, and it is doubtful that our extrapolations are any better than this. As can be seen from Table III the agreement between  $H_c$  values of specimens measured on the same run approaches the accuracy of the measuring method. This excellent agreement between pure aluminum specimens when measured together has been found to hold in a large number of similar comparison measurements.

The experimental points show appreciable deviation from the  $T^2$  relation for temperatures above about  $1.12^\circ\text{K}$ . They also begin to show more scatter. To some extent this may be due to the anomalous broadening of the transition in single crystals which makes our

criterion for determining  $H_c$  more difficult to apply as  $T \rightarrow T_c$  since the  $\mu_c$  curves become blurred and distorted. However, the uncertainty in  $H_c$  caused by this effect is only a few tenths of a gauss while the experimental points can be seen to deviate from the straight line of Fig. 6 by as much as 1.5 gauss. It would seem that uncertainty in fixing  $H_c$  is not the reason for the trend of the data near  $T_c$ , although it may be more than coincidental that the anomalous broadening and the deviation from  $T^2$  dependence occur in the same temperature interval. Although such deviations have not been described by previous investigators, there is no reason for surprise that Al should show deviation from a  $T^2$  dependence. The recent work of Goodman<sup>9</sup> on the specific heat of Al in the superconducting state has shown that it varies exponentially with  $T$ , and on thermodynamic grounds this result is incompatible with a rigorous dependence of  $H_c$  upon  $T^2$ . Of course, the critical field curve could appear parabolic to within experimental error in a limited temperature range as the present results attest.

We have indicated by the dashed line in Fig. 6 the general course of the data as  $T \rightarrow T_c$ . This dashed line extrapolates to  $H_c = 0$  at a temperature of  $1.205^\circ\text{K}$ . Logically this would seem to be the value that we should give as  $T_c$  for pure Al, but we are not entirely convinced that this is correct. Although calibrated salt pill runs were not made with polycrystalline specimens,

<sup>9</sup> B. B. Goodman, *Compt. rend.* **224**, 2899 (1957).

the comparison observations (see Fig. 5) suggest that the polycrystals would follow the parabolic temperature dependence with a smaller (or possibly no) deviation near  $T_c$ . Whether the behavior of the polycrystals or the single crystals is more intrinsically characteristic of aluminum is not clear at present, and we are inclined to regard the magnitude of  $T_c$  as uncertain within the limits set by the extrapolations of the straight and curved lines of Fig. 6.

As inspection of Table III shows, the values of  $H_c$  for two specimens on either run agrees in practically all instances to within 0.1 gauss, which is essentially the limit of resolution of the field measurement. It is readily shown from (3) that an uncertainty,  $\Delta H_c = 0.1$  gauss, is equivalent at  $1^\circ\text{K}$  to less than a millidegree uncertainty in  $T$ . This is small in comparison with the uncertainties associated with the actual measurement of  $T$  in the experiment, and we may disregard the errors in  $H_c$  in the present discussion.

The error in the temperature determinations can be considered as arising from two uncertainties: (a) the precision of a given mutual inductance reading, and (b) the uncertainty in the calibration constants of (1). The uncertainty in  $M_0$  was essentially constant at all temperatures and equal to  $\pm 0.5 \mu\text{h}$ . Using the calibration constants in (1) it may be shown that this uncertainty in  $M_0$  corresponds to a temperature uncertainty which varies from about a millidegree at  $1^\circ\text{K}$  to about 18 millidegrees at  $4^\circ\text{K}$ . A statistical analysis of the calibration data shows the constants  $A$  and  $B$  to have probable errors of about 0.1 and 0.3%, respectively, with a resultant uncertainty in  $T$  at  $1^\circ\text{K}$  of about 3.6 millidegrees. It would thus appear that the magnetic temperatures near  $1^\circ\text{K}$  are good to  $\pm 0.005\text{K}$ . Actually the error may be somewhat greater since the statistical treatment does not take into account (1) the probable error in the Curie-Weiss  $\Delta$  (which is thought to be unimportant) and (2) error associated with incomplete thermal equilibrium between the salt pill and the liquid helium bath. This second factor may be appreciable, but it is difficult to evaluate. Equilibrium times of at least 30 minutes were allowed when taking the calibration points, but in the subsequent reduction of the data a few instances were noted in which the scatter of the  $M_0$  values was greater than could be explained by the uncertainty in reading the mutual inductance. Presumably this indicates lack of thermal equilibrium.

No direct experimental check on the accuracy of our extrapolations is possible without going to much more elaborate procedures. However, if, as we believe, the critical field for pure Al is a highly reproducible thermometric parameter, the agreement between the critical-field curves obtained on the two runs shown in Fig. 6 provides an independent check on at least the self consistency of the extrapolations. The two runs were performed several months apart and analyzed separately. Temperature-wise the agreement between

the two runs ranges from complete agreement at  $T_c$  to about 8 millidegrees at  $0.8^\circ\text{K}$ , which is about the predicted uncertainty of the extrapolation.

Before leaving the question of thermometry, it is of interest to mention some results obtained with the carbon resistance thermometer which was present in the apparatus on all runs. The resistance readings were recorded for most of the calibration points and it was thus possible to determine an  $R$  versus  $T$  calibration equation. The  $R$ - $T$  relation could then be extrapolated into the superconducting temperature region and the "resistive" temperature compared with the magnetic temperature.

The procedure followed in determining the "resistive" temperature was similar to that described by Corak *et al.*<sup>10</sup> The calibration values of  $R$  and  $T$  were fitted by least squares to the Clement 2-constant equation

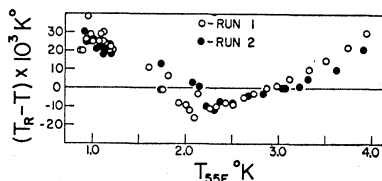
$$\frac{1}{T_R} = \frac{a^2}{\log R} + b^2 \log R + 2ab,$$

and then a correction curve was determined by plotting  $(T_R - T_{55E})$  vs  $T_{55E}$ . The correction curves for the two runs are shown in Fig. 7.† The points clustered near  $1^\circ\text{K}$  give  $(T_R - T_{\text{mag}})$  vs  $T_{\text{mag}}$  and they appear to represent a reasonable continuation of the correction curve obtained in the calibration region. It would therefore seem that by judicious extrapolation of such a correction curve, one might obtain absolute temperatures from a carbon resistor with an accuracy comparable to that achieved in the present magnetic measurements. The data of Fig. 7 also indicate that the extrapolation of an  $R$ - $T$  equation without using the correction curve can lead to substantial errors since, for all we know, the correction curve may continue to rise as  $T \rightarrow 0^\circ\text{K}$ .

### C. Supercooling and Quenching

Despite the many runs performed on the four single crystals, very little new information can be added to the discussion contained in I. The supercooled transitions were very sharp, less than 0.08 gauss wide, the

FIG. 7. The difference between temperatures determined from the resistance-temperature equation and from the  $T_{55E}$  vapor-pressure scale. Temperatures near  $1^\circ\text{K}$  were determined from magnetic measurements.



<sup>10</sup> Corak, Garfunkel, Satterthwaite, and Wexler, *Phys. Rev.* **98**, 1699 (1955).

† The rather large scatter of the data in Fig. 7 warrants the following explanation. In the present work, the carbon resistor was used primarily to indicate temperature variation rather than absolute magnitude. Accordingly, less attention was paid to such details as stabilizing the measuring voltage and balancing out thermal emf's.

TABLE IV. Summary of critical-field constants for aluminum.

Author	$H_0$ (gauss)	$T_c$ (°K)	$2H_0/T_c$ (gauss/ deg)	Technique
Daunt and Heer <sup>a</sup> together with Shoenberg <sup>b</sup>	102	$1.179 \pm 0.010^c$	173	Adiabatic demagnetization, irregular pieces of Al imbedded in salt pill. Shoenberg: Pumped liquid helium, temperature from vapor pressure over He bath corrected to 1948 scale.
Goodman and Mendoza <sup>a</sup>	106.0	$1.197 \pm 0.01$	177	Adiabatic demagnetization, measured field for which flux first penetrates specimen and corrected for demagnetizing factor of specimen. Polycrystals.
Faber <sup>d</sup>	$96 \pm 1$	$1.172 \pm 0.003$	164	Pumped liquid helium, temperature from vapor pressure over bath.
Present work				
Run 1:	97.8	$1.196 \pm 0.005$	164	Pumped liquid helium, temperature from salt pill immersed in helium bath.
Run 2:	100.0	$1.196 \pm 0.005$	167	

<sup>a</sup> J. G. Daunt and C. V. Heer, Phys. Rev. **76**, 1324 (1949).

<sup>b</sup> D. Shoenberg, Proc. Cambridge Phil. Soc. **36**, 84 (1940).

<sup>c</sup> B. B. Goodman and E. B. Mendoza, Phil. Mag. **42**, 594 (1951).

<sup>d</sup> See reference 11.

<sup>e</sup> The accuracy of this value is uncertain. See discussion in reference c.

dependence upon temperature was roughly the same for all of the single crystals and appeared, in each specimen, to be stable from run to run. Only single crystal 10 exhibited a quench effect. Before the following run this crystal was severely bent and allowed to anneal at room temperature for about 12 hours (the customary time between assembly of the apparatus and the start of a run), with the result that the quench effect disappeared.

The maximum degree of supercooling occurred near  $T_c$ , where the ratio  $H_s/H_c$  became less than 0.07, in rough quantitative agreement with Faber's work.<sup>11</sup>

Each of the polycrystals exhibited a quench field at one time or another, but neither the supercooled transition fields nor the quench fields were reproducible from run to run, although the quench effect was particularly erratic.

#### IV. DISCUSSION OF RESULTS

##### A. Critical-Field Constants

In Table IV the results of our two runs are compared with those reported by previous investigators. In listing our results we have disregarded the curving tendency of our data near  $T_c$ .

Inspection of Table IV shows the following regularities.  $H_0$  values determined in experiments where cooling was by adiabatic demagnetization are somewhat greater than when determined by extrapolation of measurements near 1°K.  $T_c$  values from the vapor pressure of liquid helium are consistently smaller than those determined by magnetic thermometry. The relative steepness of the critical-field curves as evidenced by values of  $2H_0/T_c$  (i.e., the slope at  $T_c$ ) is greater in the low-temperature measurements than in the measurements made near 1°K, but agreement between

measurements made by one or the other cryogenic technique is reasonably good.

The agreement between Faber's value of  $(dH_c/dT)T_c$  and those obtained in the present work probably reflects the superiority of a liquid-helium bath over adiabatic demagnetization techniques with respect to temperature stability and control in the range near  $T_c$ . Although appreciable differences in the absolute temperature are indicated by the  $T_c$  values, it is to be expected that the temperature differences measured by Faber and in this work will be more accurate than the absolute values themselves, and the tabulated values bear this out. We also note that the recent calorimetric data of Goodman<sup>9</sup> indicate a value of about 150 gauss/deg for  $(dH_c/dT)T_c$ . This is roughly intermediate between the most recent values given in Table IV and the value obtained from the slope of the dotted curve of Fig. 6, which represents our data best near  $T_c$  and for which  $(dH_c/dT)T_c = 142$  gauss/deg. It would thus appear that of the various constants of superconducting aluminum, at least  $(dH_c/dT)T_c$  is in reasonably good shape.

As regards the other regularities noted in Table IV, it is difficult to tell whether they are characteristic of the properties of aluminum or are indicative of systematic errors in the various measurements. Taken at face value the combined results appear to show that the critical-field curve for Al deviates from a parabolic law in the same qualitative way known to occur in the case of the elements Sn, V, In, and Tl. However, the disagreements between values in the regions where the various measurements overlap suggest either that the superconducting properties of aluminum are sensitive to the history of preparation of the specimen or that the measurements are less accurate than supposed. In this connection, we remark that in this and other work on Al in this laboratory all measurements show that the  $H_c$  vs  $T$  curve is *not* sensitive to polycrystallinity, annealing, or strains deliberately introduced at room temperature (except for the effects noted near  $T_c$ ).<sup>12</sup> On the contrary, it appears sufficiently reproducible from specimen to specimen to suggest that the superconducting transition in pure Al might make a satisfactory auxiliary thermometric standard near 1°K. We are therefore inclined to view the disagreements in the values of Table IV as primarily indicative of experimental error—in particular, the difficulty of accurate determination of the absolute temperature near 1°K. However, in view of the disagreement between the most recent determinations of  $T_c$  it would appear that additional measurements of aluminum will be required

<sup>12</sup> Strains introduced into a superconducting specimen at low temperature are another story. Various evidence indicates that strains introduced at low temperatures can produce marked effects on the superconducting transition. While such effects have not been demonstrated for Al, this is an objection which may be raised against the method of specimen preparation used by Daunt and Heer and also that of Goodman and Mendoza.

<sup>11</sup> T. E. Faber, Proc. Roy. Soc. (London) **A231**, 353 (1955).

before its critical field can be used as an accurate standard of thermometry.

### B. Transition Broadening

Transition broadening in superconductors has been observed by many experimenters and has in most cases been attributed to the effect of impurities or to strain. This does not seem to be a likely explanation for the broadening observed in the present experiments near  $T_c$  because the aluminum single crystals are of high purity and certainly have lattices which are more nearly perfect and free of residual stress than the polycrystals which do not exhibit the effect.

### C. Effective Demagnetizing Coefficient

In the appendix it is shown that owing to the existence of a surface energy between the superconducting and normal phases, the effective permeability should be roughly a linear function of  $h=H_e/H_c$ , at least for  $h$  close to unity, but with a slope corresponding to an effective demagnetizing coefficient

$$\frac{1}{n_e} = \frac{1}{n} + \frac{2.4}{n^2} \left( \frac{\Delta}{L} \right)^{\frac{3}{2}}. \quad (4)$$

$\Delta$  is a characteristic length used to specify the surface free energy between the normal and superconducting phases, and  $L$  is the length of the specimen. In Table V are listed the values of  $\Delta$  which would be required to explain the effective demagnetizing coefficients observed for the specimens reported herein, as well as for the ellipsoidal specimens investigated in I. Bardeen<sup>13</sup> has estimated that  $\Delta$  for aluminum should be of the order  $10^{-4}$  cm at temperatures low compared with the critical temperature. It would therefore appear that the difference between the observed and calculated demagnetizing coefficients can be definitely attributed to the surface free energy at the interface between superconducting and normal material. Considering the crudity of the model used to derive (14), there is probably not much point in worrying about the discrepancies between the various values calculated for  $\Delta$  in Table V, but one could be surprised by the difference between the polycrystalline and single-crystal cylinder results. The

TABLE V. Values of the surface energy parameter,  $\Delta$ , as determined from the breadth of the magnetic transition.

Specimen	Length $L$ (cm)	$n$ calculated	$n_e$ observed	$\Delta$ (cm) from Eq. (14)
Ellipsoid described in I	6.4	0.019	0.014	$9.6 \times 10^{-4}$
Single-crystal cylinders	5.1	0.0097	0.008	$1.3 \times 10^{-4}$
Polycrystalline cylinders	5.1	0.0097	0.004	$2.2 \times 10^{-3}$

<sup>13</sup> J. Bardeen, *Handbuch der Physik* (Springer-Verlag, Berlin, 1955), Vol. 15, p. 274.

difference is undoubtedly due to a difference in shape; the single crystals had rounded ends because they were grown from the melt, whereas the polycrystalline specimens had the sharp corners characteristic of the machined blanks.

### ACKNOWLEDGMENTS

We are grateful to F. E. L. Witt for his contributions in the design and construction of the apparatus used in this work, and to J. C. Wheatley for advice on problems of magnetic thermometry. R. S. Kaeser and R. W. Shaw gave important assistance in performing the experiments, and D. L. Decker and C. L. Wolff helped in reducing the thermometric data. One of us (J. F. C.) is indebted to the Graduate College of the University of Illinois for fellowship grants which provided support during the course of this work.

### APPENDIX

In order to calculate the effect of a surface free energy term on the intermediate-state behavior of a long cylinder, we shall use a model in which it is supposed that the intermediate state structure consists of long superconducting filaments imbedded in a matrix of normal material. Each filament has a circular cross section of radius  $a$ . Following the procedure of Cochran and Kaeser,<sup>14</sup> the thermodynamic potential per unit volume at constant temperature for such a structure can be written as

$$G = \frac{H_c^2}{8\pi} \left\{ \frac{h^2}{(1-n)} \frac{I}{I_0} + 1 - x + \frac{2x}{a} \Delta \right\}, \quad (A-1)$$

where  $x$  is the ratio of the volume of superconducting material to the total volume of the specimen,  $I$  is the magnetic moment per unit volume of the specimen due to the interaction of the superconducting filaments with the external field,  $I_0 = -H_e/[4\pi(1-n)]$  is the magnetic moment per unit volume of the specimen subjected to uniform field  $H_e$  when completely superconducting,  $h=H_e/H_c$  is the ratio of applied field  $H_e$  to the critical field  $H_c$ ,  $n$  is the demagnetizing coefficient for the specimen, and  $\Delta = 8\pi\alpha/H_c^2$ , where  $\alpha$  is the surface free energy per unit area of interface between superconducting and normal phases.

Expressing  $I$  in terms of  $H_e$ ,  $x$ , and  $D$ , the demagnetizing coefficient for a single superconducting filament, we obtain

$$\frac{I}{I_0} \simeq \frac{x(1-n)}{(1-nx)} \left[ 1 + \frac{(1-x)D}{(1-nx)} \right], \quad (A-2)$$

where  $D$  is assumed small and terms beyond the first power in  $D$  are neglected. Inserting (A-2) in (A-1) gives an expression for  $G$  to which we can apply the

<sup>14</sup> J. F. Cochran and R. Kaeser, *Physica* **33**, 727 (1957).

equilibrium conditions

$$(\partial G/\partial x)_{a,h} = 0, \quad (\text{A-3})$$

$$(\partial G/\partial a)_{x,h} = 0, \quad (\text{A-4})$$

to determine the equilibrium values,  $x_m$  and  $a_m$ , as a function of  $h$ .

From (A-3) we obtain

$$x_m = x_0 + \epsilon, \quad (\text{A-5})$$

where  $x_0 = (1-h)/n$ , and to first order

$$\epsilon = -\frac{h}{2n} \left[ \frac{2\Delta}{a} + \frac{(1-2x_0)}{h} D \right],$$

and from (A-4),

$$(1-x_0)(a/L)(adD/da) = 2\Delta/L. \quad (\text{A-6})$$

The demagnetizing coefficient for an ellipsoid equivalent to a cylinder having a length to diameter ratio of  $L/2a$  is, following Stoner,<sup>6</sup>

$$D = (4a^2/L^2)[\ln(L/a) - 1],$$

so that

$$a(dD/da) = (4a^2/L^2)[2 \ln(L/a) - 3].$$

Within the range of interest,  $10^{-6} < (\Delta/L) < 10^{-3}$ , the disagreeable analytic properties of  $\ln(L/a)$  may be by-passed by using the crude approximation

$$a(dD/da) = 12(a/L)^2, \quad (\text{A-7})$$

without making more than a 30% error in the correct

equilibrium value of  $a$ . From (A-6) we now obtain

$$a_m/L = [6(1-x_0)]^{-\frac{1}{2}} (\Delta/L)^{\frac{1}{2}}. \quad (\text{A-8})$$

To first order in  $\epsilon$  the equilibrium value,  $G_m$ , may now be approximated as

$$G_m = (H_c^2/8\pi)[1 - nx_0^2 + 7.3x_0(1-x_0)^{\frac{1}{2}}(\Delta/L)^{\frac{1}{2}}]. \quad (\text{A-9})$$

The magnetization is now obtained from the relation  $I = (1/nH_c)(\partial G/\partial x_0)$ , and the effective permeability,  $\mu_e$ , becomes

$$\begin{aligned} \mu_e &= 1 - nx_0 + (4\pi/H_c)I(1-n) \\ &= 1 - x_0 + \frac{7.3(1-n)(3-4x_0)}{6n(1-x_0)^{\frac{1}{2}}} \left(\frac{\Delta}{L}\right)^{\frac{1}{2}}. \end{aligned} \quad (\text{A-10})$$

The effective demagnetizing coefficient,  $n_e$ , is given by the reciprocal of the slope of  $\mu_e$ , i.e.,  $1/n_e = d\mu_e/dh = -(1/n)d\mu_e/dx_0$ . Since the validity of this treatment is limited to small values of  $x_0$  (i.e., near  $\mu_e = 1$ ) we evaluate  $d\mu_e/dx_0$  in the limit as  $x_0 \rightarrow 0$  with the result that

$$\frac{n}{n_e} = 1 + \frac{2.4}{n} \left(\frac{\Delta}{L}\right)^{\frac{1}{2}}. \quad (\text{A-11})$$

An alternate model of the intermediate-state structure assumes the superconducting regions to consist of laminar strips of small thickness. The method of reference 14 applied to this model always gives a higher value of  $G_m$  than is obtained for the filamented model treated in the foregoing.